



HAL
open science

Atomic arrangement at ZnTe/CdSe interfaces determined by high resolution scanning transmission electron microscopy and atom probe tomography

Bastien Bonef, Lionel Gérard, Jean-Luc Rouvière, Adeline Grenier, Pierre-Henri Jouneau, Edith Bellet-Amalric, Henri Mariette, Régis André, Catherine Bougerol

► To cite this version:

Bastien Bonef, Lionel Gérard, Jean-Luc Rouvière, Adeline Grenier, Pierre-Henri Jouneau, et al.. Atomic arrangement at ZnTe/CdSe interfaces determined by high resolution scanning transmission electron microscopy and atom probe tomography. Applied Physics Letters, 2015, 106 (5), pp.051904. 10.1063/1.4907648 . hal-01132475

HAL Id: hal-01132475

<https://hal.science/hal-01132475>

Submitted on 26 May 2021

HAL is a multi-disciplinary open access archive for the deposit and dissemination of scientific research documents, whether they are published or not. The documents may come from teaching and research institutions in France or abroad, or from public or private research centers.

L'archive ouverte pluridisciplinaire **HAL**, est destinée au dépôt et à la diffusion de documents scientifiques de niveau recherche, publiés ou non, émanant des établissements d'enseignement et de recherche français ou étrangers, des laboratoires publics ou privés.

Atomic arrangement at ZnTe/CdSe interfaces determined by high resolution scanning transmission electron microscopy and atom probe tomography

Cite as: Appl. Phys. Lett. **106**, 051904 (2015); <https://doi.org/10.1063/1.4907648>

Submitted: 10 December 2014 . Accepted: 26 January 2015 . Published Online: 04 February 2015

Bastien Bonafant, Lionel Gérard, Jean-Luc Rouvière, Adeline Grenier,  Pierre-Henri Jouneau, Edith Bellet-Amalric, Henri Mariette, Régis André, and Catherine Bougerol



View Online



Export Citation



CrossMark

ARTICLES YOU MAY BE INTERESTED IN

[High spatial resolution correlated investigation of Zn segregation to stacking faults in ZnTe/CdSe nanostructures](#)

Applied Physics Letters **112**, 093102 (2018); <https://doi.org/10.1063/1.5020440>

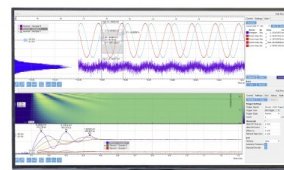
[Study of reconstruction at interfaces of CdSe/ZnTe superlattices by total energy calculations](#)
Journal of Vacuum Science & Technology B: Microelectronics and Nanometer Structures Processing, Measurement, and Phenomena **13**, 1711 (1995); <https://doi.org/10.1116/1.587882>

[Highly strained AIAs-type interfaces in InAs/AlSb heterostructures](#)

Applied Physics Letters **108**, 211908 (2016); <https://doi.org/10.1063/1.4952951>

Challenge us.

What are your needs for periodic signal detection?



Zurich Instruments



Atomic arrangement at ZnTe/CdSe interfaces determined by high resolution scanning transmission electron microscopy and atom probe tomography

Bastien Bonafant,^{1,2} Lionel Gérard,^{1,3} Jean-Luc Rouvière,^{1,2} Adeline Grenier,^{1,4} Pierre-Henri Jouneau,^{1,2} Edith Bellet-Amalric,^{1,2} Henri Mariette,^{1,3} Régis André,^{1,3} and Catherine Bougerol^{1,3}

¹Université Grenoble Alpes, F-38000 Grenoble, France

²CEA, INAC-SP2M, F-38054 Grenoble, France

³CNRS, Inst. NEEL, F-38042 Grenoble, France

⁴CEA, LETI, MINATEC Campus, F-38054 Grenoble, France

(Received 10 December 2014; accepted 26 January 2015; published online 4 February 2015)

High resolution scanning transmission electron microscopy and atom probe tomography experiments reveal the presence of an intermediate layer at the interface between two binary compounds with no common atom, namely, ZnTe and CdSe for samples grown by Molecular Beam Epitaxy under standard conditions. This thin transition layer, of the order of 1 to 3 atomic planes, contains typically one monolayer of ZnSe. Even if it occurs at each interface, the direct interface, i.e., ZnTe on CdSe, is sharper than the reverse one, where the ZnSe layer is likely surrounded by alloyed layers. On the other hand, a CdTe-like interface was never observed. This interface knowledge is crucial to properly design superlattices for optoelectronic applications and to master band-gap engineering. © 2015 AIP Publishing LLC. [<http://dx.doi.org/10.1063/1.4907648>]

II–VI semiconductors as well as their heterostructures have been intensively studied due to their promising optical properties related to their wide and direct band gap. Among them, ZnTe and CdSe have very close lattice parameters ($a = 0.6103$ nm and 0.6078 nm, respectively) in their cubic zinc-blende structure. Such a small lattice parameter mismatch of only 0.3% makes this couple a good candidate to grow almost strain-free superlattices (SLs). Furthermore, as is common in binary compound semiconductors which do not share the same anion, these SLs present a staggered band alignment¹ providing so-called type-II quantum structures for which electrons and holes are not confined in the same material. Then the optical properties of the SLs can cover a large range of energy when varying their period, even below the energy of the constituent bandgap, and the type-II effect can give rise to a straight forward spatial separation of electrons and holes, if needed.

Recently, short period ZnTe/CdSe SLs have proven to be efficient sun light absorbers² and benefit from their type-II band alignment to extract photo-generated charge carriers at their boundaries. However, the ZnTe/CdSe interface is made complex by the simultaneous change of group II and group VI elements. Even when grown by molecular beam epitaxy (MBE), which is the technique of choice to achieve semiconductor heterostructures with flat and sharp interfaces, the CdSe/ZnTe interfaces have intrinsically a finite extension, either ZnSe-like or CdTe-like; but more complex cases involving ternary or quaternary alloys or exchanges of cationic or anionic planes could be envisaged. Furthermore, the optical properties of the SLs are highly sensitive to details at the interfaces, especially when short periods are required, as recently calculated.² This phenomenon is of course not restricted to II–VI heterostructures; in particular, it has been recently studied in the case of III–V SLs with no atom in common such as InAs/AlSb³ or InAs/GaSb^{4–6} grown for quantum

cascade lasers or Mid-IR detectors, respectively, since the nature of the interfaces has a strong impact on the performances of the devices. Coming back to CdSe/ZnTe, the presence of interfacial regions involving 2–3 monolayers, distinct from ZnTe and CdSe themselves, was indeed already observed by transmission electron microscope (TEM) by Luo *et al.*,⁷ who reported in 1991 the first growth of ZnTe/CdSe SL by MBE. However, the exact nature of these regions was not determined. Later on, Kemner *et al.*^{8,9} performed EXAFS studies on these SLs and concluded, from analysis of Zn–Se and Cd–Te coordination numbers, that the ZnSe-like and CdTe-like interfaces were not sharp but could involve exchange of cations or anions; these two possibilities could not be distinguished. This model was supported by first principles pseudopotential studies¹⁰ and electronic structure calculations,¹¹ but no direct proof from imaging has been reported so far. Considering the large improvement in spatial resolution due to the development of aberration-corrected transmission electron microscopes in the last ten years, we found worthwhile to re-investigate this interface problem which becomes crucial in case of short period SLs for photovoltaic applications. This has motivated us to carry out atomic scale structural investigations of ZnTe/CdSe SLs from high resolution scanning transmission electron microscopy (HR-STEM). This was combined with atom probe tomography (APT) which enables the chemical mapping of atoms with a sub-nm spatial resolution.^{12,13} We have observed that both interfaces are not as sharp as expected in an abrupt model and that both involve ZnSe. Moreover, CdSe on ZnTe interface is wider than ZnTe on CdSe due to the presence of additional ternary or quaternary alloy layers. Finally, CdTe is never observed. This behavior is discussed in terms of cohesive energy.

The present study has been performed on two dedicated ZnTe/CdSe SLs grown by MBE. The two binary compounds were grown following standard conditions, i.e., Zn excess

for ZnTe and Se excess for CdSe. Finally, the SLs were capped with a 30 nm CdSe layer. With a view to obtain reproducible interfaces, at the end of each ZnTe layer, the surface was exposed successively to Te and then Cd before proceeding with CdSe. Similarly, at the end of each CdSe layer, the surface was exposed successively to Cd and then Te before proceeding with the next ZnTe layer. APT experiments have been carried out using a Cameca Flextap equipment operated with a green laser (515 nm). Analyses were made at 20 K to minimize surface migration of the atoms that may deteriorate the spatial resolution.¹⁴ In order to perform quantitative analyses on ZnTe/CdSe SLs, the laser energy was chosen by doing preliminary experiments on 1 μm thick ZnTe and CdSe bulk layers, with the objective to achieve a cation/anion ratio equal to one. Optimum laser energies for ZnTe and CdSe evaporation were found to correspond to a charge state ratio equal to 0.06 ± 0.02 for $\text{Zn}^{++}/\text{Zn}^+$ and 0.38 ± 0.04 for $\text{Cd}^{++}/\text{Cd}^+$. Subsequently, for the experiments on ZnTe/CdSe SLs, the laser energy was tuned to obtain these respective charge state ratios. To perform APT experiments, samples consisting of ZnTe/CdSe SLs of 12.0/9.0 nm thickness grown on InAs substrate, were prepared as tips by focussed ion beam (FIB) on a FEI Strata 400S dual beam instrument (sample 1). High resolution Z-contrast images have been acquired in STEM mode with a high angle annular dark field (HAADF) detector using a doubled corrected FEI Titan³ microscope operated at 200 kV. The samples were prepared in cross section by mechanical polishing followed by Ar ion milling. For that experiment, SLs were grown on a ZnTe (001) substrate because it has the same hardness as the SL which enables better quality samples after polishing (sample 2).

Figure 1 shows a high magnification Z-contrast image of sample 2 taken along the [110] zone axis. In this imaging mode, the contrast is directly related to the number of

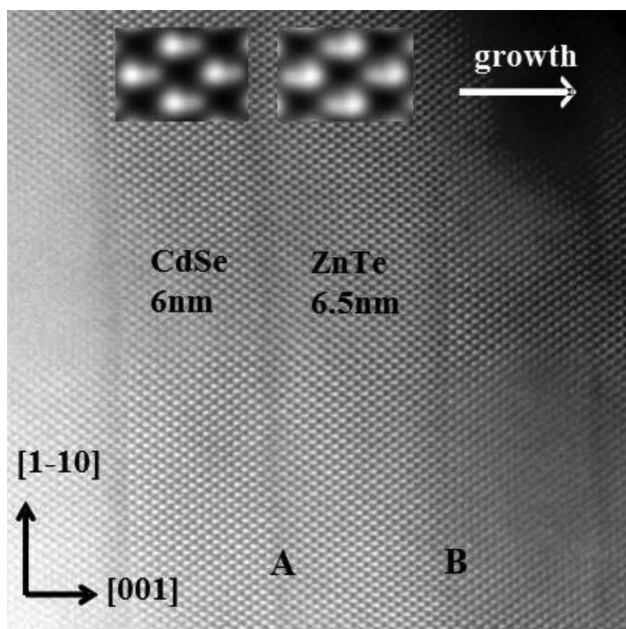


FIG. 1. HAADF-STEM image of sample 2 taken along the [110] zone axis. The two zooms given in the insets evidence the dumbbells, either (Zn,Te) or (Cd,Se). The interfaces ZnTe on CdSe and CdSe on ZnTe are labelled A and B, respectively.

electrons ($Z^{1.7}$).¹⁵ We observe that the average contrast in ZnTe and CdSe regions is similar, in agreement with the fact that ZnTe and CdSe have an equivalent number of electrons ($Z_{\text{Cd}} = 48$, $Z_{\text{Se}} = 34$, $Z_{\text{Zn}} = 30$, and $Z_{\text{Te}} = 52$). On the other hand, a dark contrast appears at each interface, compatible with the presence of lighter elements as ZnSe, whereas no bright line is seen which rules out the presence of CdTe (higher average number of electrons). In this projection of the structure, the closest atomic columns of cations and anions form dumbbells, which can be clearly resolved on the image zooms given in the inset. The respective brightness of the two dots forming the dumbbell in the ZnTe substrate (low brightness, high brightness) (later referred as (low,high)) and in the CdSe capping layer (high,low), whose images are not shown here, allows to identify unambiguously the SL layers. The dumbbell intensity analysis has been also performed at the interfaces. A zoom of the ZnTe on CdSe interface (called interface A) is given in Figure 2(a). Two profiles, taken at positions 1 and 2 marked on the image, are shown in Figures 2(b) and 2(c). In Figure 2(c), an abrupt change from a (high,low) configuration to a (low,high) one is observed, compatible with a CdSe/ZnTe sequence. However, in Figure 2(b), an additional dumbbell (low,low) is present in between (high,low) and (low,high) pairs, which can be associated with ZnSe. From such profiles, a structural model of the ZnTe on CdSe interface can be proposed, whose projection along [110] direction is given in Figure 3(a). It appears that the interface consists of 1.5 ZnSe monolayer (ML) (i.e., involving 3 Zn-Se bonds) which is formed by the 1 ML period delayed change in anionic species (Te for Se) compared to the change in cationic ones (Zn for Cd). By comparison, the sharpest possible interface would be 0.5 ML wide. The same profile analysis has been applied to the CdSe on ZnTe interface (called

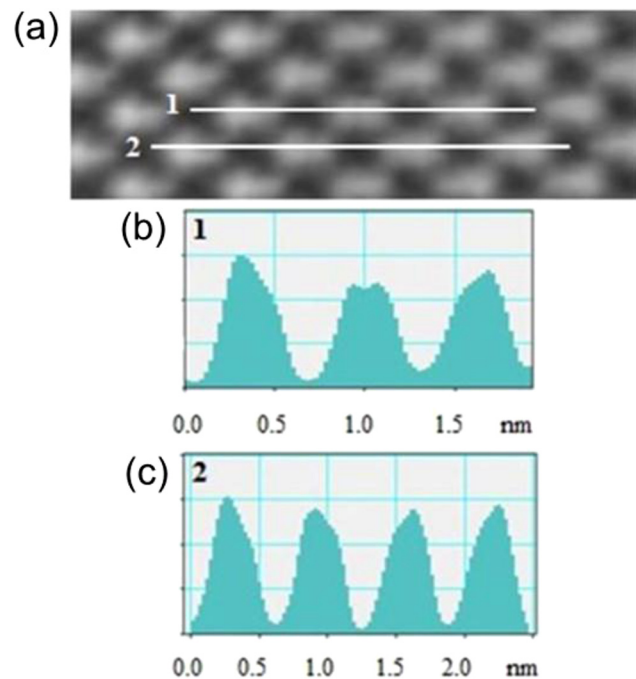


FIG. 2. (a) HAADF-STEM image of the ZnTe on CdSe interface (A) (b) Intensity profile along the line marked 1 in Figure 2(a), in the growth direction. (c) Intensity profile along the line marked 2 in Figure 2(a), in the growth direction.

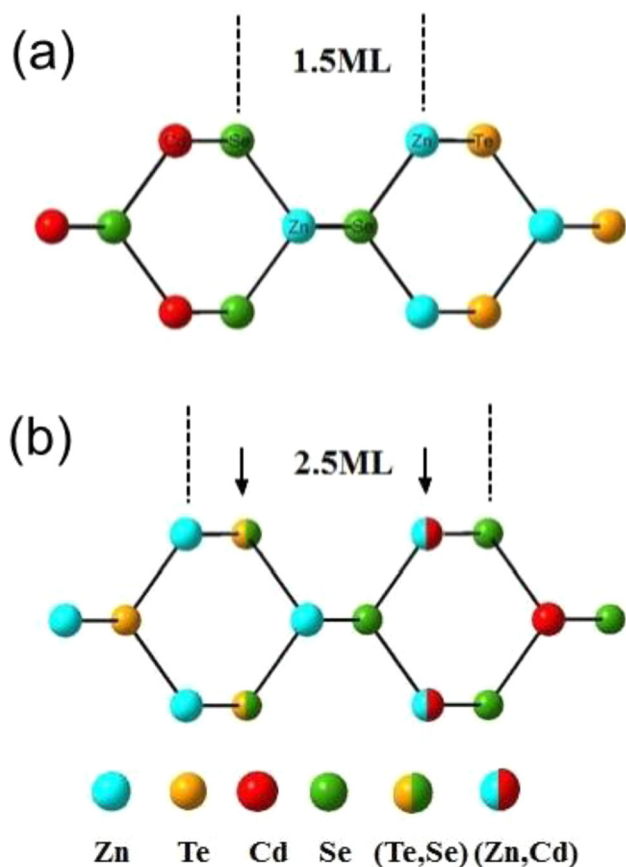


FIG. 3. Structural model projected along [110] for: (a) ZnTe on CdSe interface (A), (b) CdSe on ZnTe interface (B); the black arrows indicate the layers having cationic or anionic alloying.

interface B) and is shown in Figure 4. From the 2 profiles (Figures 4(b) and 4(c)), it appears that interface B is wider than A, due to additional layers likely consisting of ternary or quaternary alloys on each side of the ZnSe layer: Figure 4(c) involves 1 dumbbell (low,low) compatible with ZnSe between ZnTe and CdSe ones (compared to abrupt change for interface A); Figure 4(b) includes two dumbbells between ZnTe and CdSe (compared to 1 ZnSe dumbbell for interface A), whose intensities likely reflect an alloying of anions or cations such as (Zn,Se + Te) and (Zn + Cd,Se). Although it is not possible to go further in the chemical description of this interface, the transition region is obviously wider than for the inverted one (2.5 versus 1.5 ML), as can be seen on the structural model shown in Figure 3(b). Moreover, it is clear that no (high,high) dumbbell appears, which rules out the hypothesis of a CdTe interface.

To add a chemical insight to the contrast analysis presented above, samples were investigated by APT. The atom probe volume was reconstructed using the voltage based algorithm reported by Gault *et al.*¹⁶ The low differences in evaporation field between ZnTe and CdSe allows the reconstruction of layers with the expected thicknesses and flat interfaces. Figures 5(a) and 5(b) show a 3D reconstruction of the atomic distribution and concentration profiles for sample 1. These are drawn perpendicularly to the interfaces, and the concentrations are measured by counting atoms in sampling boxes of $10 \times 10 \times 0.2 \text{ nm}^3$ with a moving step of 0.2 nm. We notice a good agreement with a 1/1 cation/anion ratio for

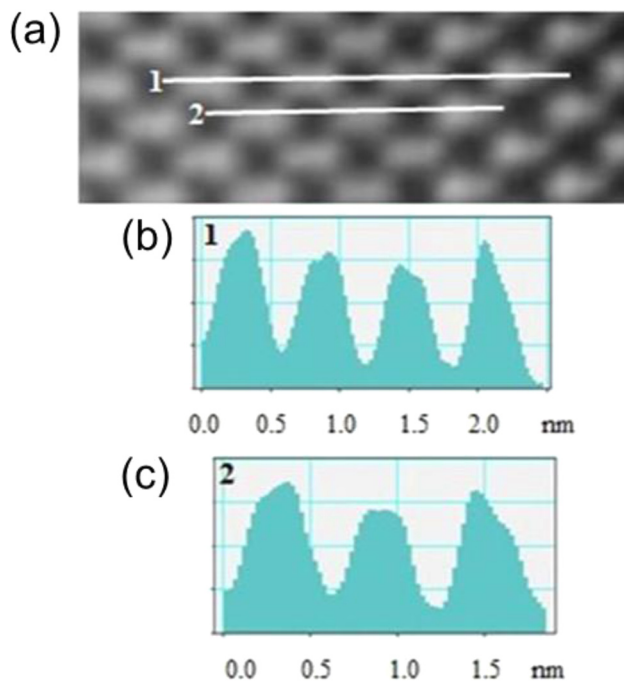


FIG. 4. (a) HAADF-STEM image of the CdSe on ZnTe interface (B). (b) Intensity profile along the line marked 1 in Figure 4(a), in the growth direction. (c) Intensity profile along the line marked 2 in Figure 4(a), in the growth direction.

both ZnTe and CdSe layers. From these profiles, all interfaces appear broader, namely, around 6 ML wide, than from HAADF-STEM images analyses and it is therefore not possible to confirm the asymmetry, 1.5 ML vs 2.5 ML, mentioned above. The spatial resolution of the atom probe is poorer than the aberration-corrected STEM image as previously observed on III-V semiconductors.⁵ More interestingly, the mass spectrum revealed the presence of molecular ions having a mass range corresponding to ZnSe^+ (Figure 5(c)), which were found to originate from each interface (Figure 5(d)). This is in perfect agreement with the description of the interfaces from HAADF-STEM images. On the other hand, no sign of CdTe was detected, which cannot be assigned to an experiment artefact since CdTe^+ and CdTe^{2+} molecular ions were observed when a CdTe tip was evaporated in the same experimental conditions.

The predominant formation of ZnSe at the interfaces can be explained by the difference in cohesive energies between the four cation/anion couples: -2.69 eV , -2.52 eV , -2.36 eV , and -2.18 eV for ZnSe, CdSe, ZnTe, and CdTe, respectively.¹⁷ When switching from Cd + Se to Zn + Te fluxes, the strongest ZnSe bonds would form preferentially as long as Se residual atoms were present in the chamber, leading to a delay for Te incorporation. In the opposite case, CdTe would not form as the CdTe bond is the weakest. A similar situation has been reported recently in the case of III-V InAs/AlSb interfaces by Nicolai *et al.*³ who observed the predominant formation of AlAs-like interfaces assigned to the high thermal stability of AlAs.

To conclude, we have shown from HR-STEM and APT experiments, the presence of an intermediate layer at the interface between two binary compounds with no atom in common, namely, ZnTe and CdSe, for samples grown by

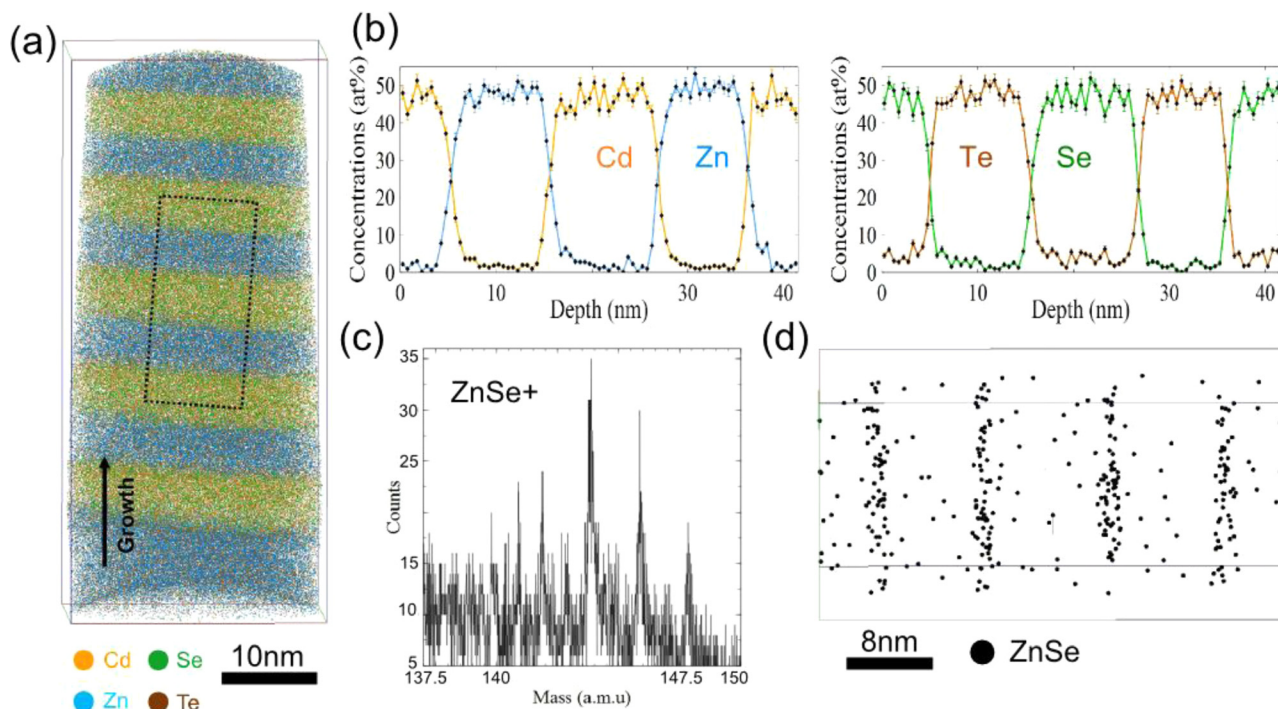


FIG. 5. (a) 3D reconstruction of the atomic distribution from APT performed on sample 1. The colors blue, orange, brown, and green refer to Zn, Cd, Te, and Se, respectively. (b) Concentration profiles of the corresponding atomic species. (c) Mass spectrum of sample 2 focused on ZnSe⁺. (d) Spatial reconstruction showing that ZnSe⁺ molecular ions originate from the interfaces.

MBE under standard conditions. This thin transition layer, of the order of 1 to 3 atomic planes, contains typically one monolayer of ZnSe. Even if it occurs at each interface, it is worth noting that a clear difference between the direct, ZnTe on CdSe, and the reverse interface. The direct interface is sharper, whereas for the reverse interface, the ZnSe layer is likely surrounded by alloyed layers. This knowledge is crucial to properly design SLs for optoelectronic applications and to master band-gap engineering. For instance, the unexpected ZnSe layer exhibits a bandgap of 2.8 eV instead of 2.4 and 1.7 eV for ZnTe and CdSe, respectively. The presence of alloy layers at the CdSe/Te and ZnTe/Se interfaces must also be considered since CdSeTe and ZnTeSe alloys are known to exhibit strong non-linearity of their band-gap versus composition, with values lower than that of both their constituents.^{18,19} To go further and make the best ZnTe/CdSe SL, one has to take into account the detailed reality of the interfaces or to eventually modify the growth conditions and force a different interface if necessary. For example, in the case of SL optimized for sun absorption in a photovoltaic context, it was shown theoretically that CdTe interfaces would be favorable to match the solar spectrum.²

¹D. Mourad, J.-P. Richters, L. Gérard, R. André, J. Bleuse, and H. Mariette, *Phys. Rev. B* **86**, 195308 (2012).

²S. Boyer-Richard, C. Robert, L. Gérard, J.-P. Richters, R. André, J. Bleuse, H. Mariette, J. Even, and J.-M. Jancu, *Nanoscale Res. Lett.* **7**, 543 (2012).

³J. Nicolai, C. Gatel, B. Warot-Fonrose, R. Teissier, A. N. Baranov, C. Magen, and A. Ponchet, *Appl. Phys. Lett.* **104**, 031907 (2014).

⁴E. Luna, F. Ishikawa, B. Satpati, J. B. Rodriguez, E. Tournié, and A. Trampert, *J. Cryst. Growth* **311**, 1739 (2009).

⁵H. Kim, Y. Meng, J. L. Rouvière, D. Isheim, and D. Seidman, *J. Appl. Phys.* **113**, 103511 (2013).

⁶K. Mahalingam, H. J. Haugan, G. J. Brown, and K. G. Eyink, *Ultramicroscopy* **127**, 70 (2013).

⁷H. Luo, N. Samarth, F. C. Zhang, A. Pareek, M. Dobrowoiska, and J. K. Furdyna, *Appl. Phys. Lett.* **58**, 1783 (1991).

⁸K. M. Kemner, B. A. Bunker, H. Luo, N. Samarth, J. K. Furdyna, M. R. Weidmann, and K. E. Newman, *Phys. Rev. B* **46**(11), 7272 (1992).

⁹K. M. Kemner, B. A. Bunker, A. J. Kropf, H. Luo, N. Samarth, J. K. Furdyna, M. R. Weidmann, and K. E. Newman, *Phys. Rev. B* **50**(19), 14327 (1994).

¹⁰S.-F. Ren, Z.-Q. Gu, and Y.-C. Chang, *J. Vac. Sci. Technol. B* **13**(4) 1711 (1995).

¹¹J. Yu, M. Bing-Xian, S. San-Guo, and Y. Shi-E, *Acta. Phys. Sin.* **8**(1), 46 (1999).

¹²B. Gault, F. Vurpillot, A. Vella, M. Gilbert, A. Menand, D. Blavette, and B. Deconihou, *Rev. Sci. Instrum.* **77**, 043705 (2006).

¹³D. J. Larson, T. J. Prosa, R. M. Ulfing, B. P. Geiser, and Th. F. Kelly, *Local Electrode Atom Probe Tomography* (Springer, 2013).

¹⁴B. Gault, M. Müller, A. La Fontaine, M. P. Moody, A. Shariq, A. Cerezo, S. P. Ringer, and G. D. W. Smith, *J. Appl. Phys.* **108**, 044904 (2010).

¹⁵S. J. Pennycook, *Ultramicroscopy* **30**(1-2), 58 (1989).

¹⁶B. Gault, M. Moody, J. Cairney, and S. Ringer, *Atom Probe Microscopy* (Springer, New York, 2012), pp. 169–171.

¹⁷X. W. Zhou, D. K. Ward, J. E. Martin, F. B. van Swol, J. L. Cruz-Campa, and D. Zubia, *Phys. Rev. B* **88**, 085309 (2013).

¹⁸C. Uzan, H. Mariette, and A. Muranevich, *Phys. Rev. B* **34**(12), 8728 (1986).

¹⁹M. J. S. P. Brasil, R. E. Nahory, F. S. Turco-Sandhoff, H. L. Gilchrist, and R. J. Martin, *Appl. Phys. Lett.* **58**(22), 2509 (1991).